

Anisotropic 2.5D Inversion of Towed Streamer EM Data from Three North Sea Fields Using Parallel Adaptive Finite Elements

K. Key (Scripps Institution of Oceanography), Z. Du* (PGS), J. Mattsson (PGS), A. McKay (PGS) & J. Midgley (PGS)

SUMMARY

We present anisotropic inversion results from towed streamer electromagnetic (EM) surveys of the Bressay, Bentley and Kraken (BBK) heavy oil fields in the North Sea. The BBK discoveries pose several challenges to conventional controlled-source EM surveying since the relatively shallow water dampens the anomaly magnitudes due to airwave coupling, and the reservoirs are in close proximity to other resistive features. The 160 m spacing of the 44 receiver bipoles on the towed streamer offers much higher data density than is typically achieved with conventional seafloor receiver surveys. We tested the resolving capabilities of the towed-streamer by inverting the survey data using a new code based on a 2.5D parallel goal-oriented adaptive finite element method and a modified implementation of the Occam inversion algorithm. The inversion successfully images the 1-2 km wide Bressay and ~5 km wide Bentley reservoirs, illustrating that the high data density of the towed streamer offers improved resolution over sparsely sampled nodal seafloor receiver data. The results also demonstrate the importance of allowing for anisotropy when inverting data from this region. Whereas anisotropic inversion clearly recovers the lateral edges of the known reservoirs, isotropic inversion results in inter-bedding of resistive and conductive layers that conceal the reservoirs.

Introduction

In 2012 PGS conducted a challenging survey in a complex geological region over Bressay, Bentley and Kraken (BBK) heavy oil fields in the North Sea (Figure 1) using the newly developed controlled-source Towed Streamer EM acquisition system. The towed system consists of a ~ 7.7 km receiver cable deployed at 50 -100 m water depth, and a powerful (1,500 A) 800 m long bipole source towed at 10 m depth. Using a 4 knot tow-speed, the acquisition pattern was based on a source signal every 250 m and 44 unique receiver positions for each “shot”. Compared to a conventional node-based marine controlled-source electromagnetic (CSEM) system, where the receivers are very sparsely placed on the seafloor in a line or areal pattern, approximately 1 km apart, the highly sensitive receiver electrodes housed in the streamer of the towed EM system are able to densely sample the subsurface with an average offset interval of ~ 160 m over offset ranges of 800 to 7595 m. The Towed Streamer EM system thus provides the dense sampling, data quality and signal-to-noise ratio required for imaging challenging targets in a shallow water environment.

The BBK discoveries were considered to pose several challenges to conventional CSEM surveying since relatively shallow water depths dampen the EM anomaly magnitudes due to airwave coupling, and the known reservoirs lie in close depth proximity to highly resistive basement formations. Figure 1 shows a map of the survey region and the 8 EM profiles, ranging in length from 9 km to 63 km. The final processed data set consists of six discrete transmission frequencies (0.2, 0.4, 0.6, 0.8, 1, 1.2 Hz) recorded by all 44 receivers for transmitter bins spaced every 250 m along the survey profiles.

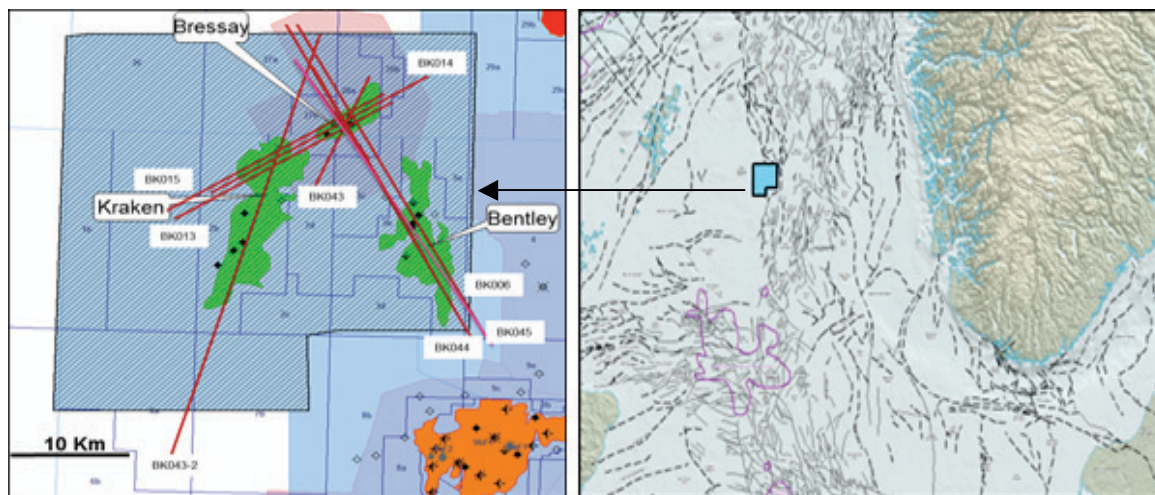


Figure 1. Map showing the towed-EM survey profiles (red lines) collected in 2012 over the Bentley, Bressay and Kraken reservoirs in the North Sea.

Inversion using 2.5D parallel adaptive finite elements

The BBK data was inverted using the open-source program MARE2DEM, which is a regularized non-linear 2.5D inversion built around a parallel adaptive finite element algorithm (Key, 2012). The finite element approach uses automatic mesh generation and goal-oriented adaptive refinement to generate a mesh that is accurate for a given suite of data and model parameters. Non-linear inversion is carried out using the Occam method (Constable et al., 1987), a regularized variant of Gauss-Newton minimization that automatically determines a suitable trade-off parameter during each iteration. While the main Occam methodology is followed, MARE2DEM leverages a version of the golden-section search algorithm that was modified to abort each iteration’s minimization search if a given test model’s misfit drops below a threshold that is some fraction of the initial model misfit. This results in much fewer forward evaluations than are required when the complete golden section search is exercised. A threshold of about 85% typically results in Occam finding a good fitting model in 25-40% less time.

Parallelization of the forward code is accomplished with a manager-worker approach implemented with the Message Passing Interface (MPI) library standard. Since the adaptive finite element mesh density and hence computational run time for a given modeling task depends on the number of transmitters and receivers, MARE2DEM performs the adaptive finite element calculations on many small subsets of transmitters and receivers in parallel, rather than attempting to model all of them with a single adaptively refined mesh of much greater density. A queue on the manager processor is used to store all the data subset modeling tasks so that when a given worker completes a task, the next task in the queue is assigned to that worker. For a typical CSEM modeling problem, the number of independent modeling tasks can range from hundreds to thousands, hence our parallel approach to the forward code scales very efficiently when run on a few hundred processors.

Parallelization of the dense matrix multiplications and factorizations required by the Occam inversion algorithm is accomplished with the ScaLAPACK library, a subset of the LAPACK linear algebra routines that has been coded for distributed computing using all processors on a cluster. As an example of the performance increase possible, consider a problem with 30,000 unknown model parameters; the dense matrix operations required several tens of minutes when using the serial LAPACK routines on a single processor but were reduced to only 30 seconds when run in parallel on 200 processors using ScaLAPACK.

At offset ranges less than about 4 km, the 800 m long transmitter dipole wires and 200 to 1098 m long receiver dipoles measure electromagnetic fields that depart significantly from those of point dipoles due to bipole effects. We modified MARE2DEM to include these effects by evaluating a line integral of the EM responses produced by a continuum of point dipoles situated along a given dipole wire. Therefore, we refer the towed system source and receivers as bipoles. Since the EM fields vary smoothly as a function of position in the seawater, this integral can be numerically approximated using a low-order Gauss-Legendre quadrature rule (e.g., Trefethen, 2000). For the towed-streamer configuration, we found that an order $n=3$ quadrature rule results in 1% or better accuracy at all streamer offsets. Since the number of transmitter and receiver point dipole pairs to be modeled increases by a factor of n^2 , this approach increases the computational burden by a factor of 9.

Another challenge when modeling towed streamer data is the significant increase in data density compared to conventional nodal seafloor receiver surveys. The towed streamer data contains source signals spaced every 250 m, each with 44 unique receiver channels spaced with an average interval of 160 m. For a 30 km tow line there will be 120 transmitter positions and 5280 data points per frequency. In comparison, conventional seafloor receiver data typically has receiver nodes spaced every 1000 m. If the receivers only measure data to 8 km offset, a 30 km long tow-line will have about 12 receivers per transmitter (given in and out-tow geometries and accounting for receivers at ends of the line). Assuming a similar 250 m transmitter stack bin, the seafloor receiver-node profile will have only 1440 data per frequency. Thus, a towed streamer profile has about four times the data density as a typical seafloor receiver survey. While in principle this difference could be eliminated by deploying seafloor receivers every 160 m, in practice deploying the necessary 188 seafloor receivers would consume a significant amount of time, especially when considering this is only a single 30 km profile. The computational burden of this increased data density is further compounded by the fact that the usual trick of using reciprocity to lighten the computational load (by interchanging the modelled transmitter and receiver dipoles) is not possible since the towed receivers move with the transmitter.

Inversion of the data from Bentley, Bressay and Kraken

For the MARE2DEM inversions, we parameterized the model domain with a dense grid of around 10,000-20,000 unknown resistivity parameters (depending on the profile length) from the seafloor to 2 km depth. We applied a 1% error floor to the data and found that most of the survey profiles could be fit to a root-mean-squared (RMS) misfit of about 0.8 to 1.0 within about 10-15 Occam iterations, requiring a few hours of run-time on 160 processors. An initial blind (without considering field

geology) inversion for isotropic resistivity resulted in strong horizontal bands of alternating resistive and conductive layers, with some evidence for increased resistivity at the locations of the reservoirs near 1 km depth. Figure 2(a) shows an example isotropic inversion result for profile BK006.

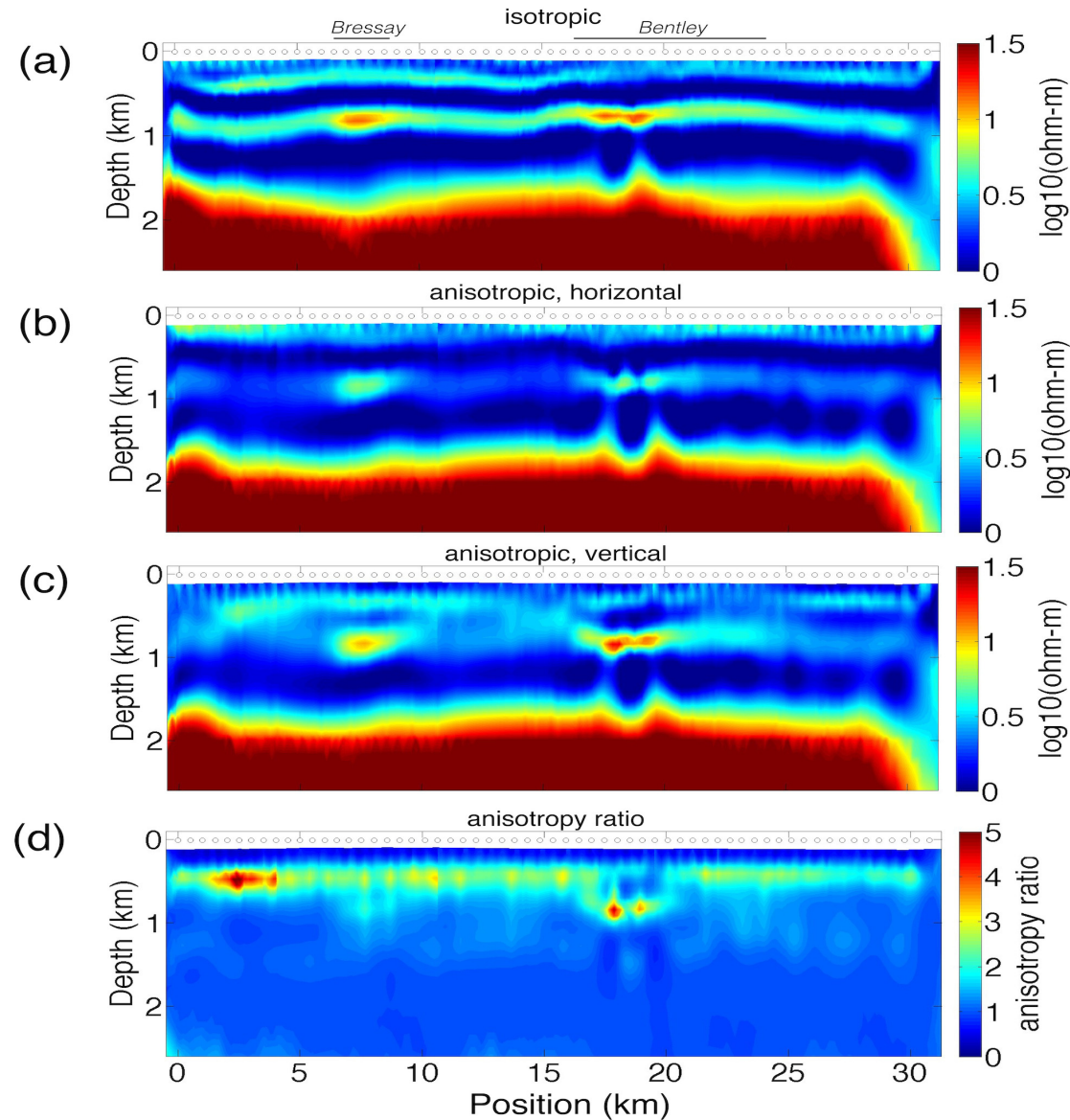


Figure 2 Example MARE2DEM inversions for profile BK006. Isotropic inversion (a) shows significant horizontal bands of high resistivity that mask the presence of the two reservoirs. Anisotropic inversion for the horizontal (b) and vertical (c) resistivity clearly images the discrete reservoir resistors. The vertical/horizontal anisotropy ratio (d) shows that anisotropy reaches a factor of 3 in a ubiquitous layer at 0.5 km depth. The charged reservoirs are also seen to be anisotropic.

Since nearby well logs and the field geology suggested that the sediments outside the reservoirs shouldn't be as resistive as indicated by the inversion model, we decided to test whether the stripes may be indicative of anisotropic effects (e.g., Newman et al., 2010). Our first test consisted of an isotropic inversion of synthetic data from a model containing sediments with 1.0 ohm-m horizontal and 1.5 ohm-m vertical resistivity. The resulting inversion showed similar stripes to that shown in Figure 2a, suggesting that the stripes in the real inversion are likely just an artifact of creating effective anisotropy by means of introducing isotropic layers of different resistivity. Hence we abandoned the isotropic inversions in favor of anisotropic inversion. We augmented the inversion's model roughness penalty with an additional penalty against anisotropy, so that anisotropy should only appear where required to fit the data. The resulting horizontal and vertical resistivity components for

profile BK006 are shown in Figures 2b & 2c respectively. The anisotropic inversion clearly resolves the presence of the Bentley and Bressay reservoirs, and does not contain the significant horizontal layering observed in the isotropic inversion. Note the diffusive nature of EM fields means that the unconstrained inversion is not sensitive to the difference between sharp boundaries and more gradual changes. Although such details are not rigidly constrained, as shown in Figure 2, the lateral extensions of the Bentley and Bressay reservoirs are in good agreement with the main target geometries as defined by seismic imaging. Figure 2(d) shows the anisotropy ratio for this inversion, which reveals a ubiquitous layer at ~ 0.5 km depth that displays a factor three anisotropy ratio, whereas the rest of the model, except the reservoirs, is nearly isotropic (ratio equal to one). The significant shallow anisotropy is most likely caused by the inter-bedding of shale with brine sand in the overburden, as suggested by nearby log analysis.

Interpretation of CSEM data proceeds in stages, starting with unconstrained inversions that provide a broad class of structures to which the data are sensitive. More fine-scale structural detail can be introduced into the inversion through the use of boundary constraints from seismic imaging. In parallel with this study, Du and Hosseinzadeh (2014) have derived a 2.5D seismic guided EM inversion, based on the anisotropic inversion presented here. By doing this the resolution of the resulting resistivity model has dramatically improved compared to the unconstrained inversion result, and the properties of the resulting model are more accurately estimated.

Conclusions

Our inversion studies of towed streamer EM data from the BBK region clearly illustrate the importance of including anisotropy in inversion models. When the inversion is restricted to isotropic resistivity, the recovered model contains strongly alternating stripes of resistive and conductive layers that conceal the known reservoirs. Conversely, anisotropic inversion recovers more uniform sedimentary features and clearly maps the lateral edges of the reservoirs. Since both the isotropic and anisotropic models fit the data equally well, we cannot recommend one approach over the other from a misfit point of view. However, the anisotropic inversion results present a more plausible geological scenario. Hence it is our preference. The detection of the 1-2 km wide Bentley reservoir illustrates that the high data density of the towed-EM streamer can image much narrower resistive structures than are usually considered possible with conventional CSEM data collected using seafloor receivers.

Acknowledgements

We thank PGS for the permission to publish this work. K. Key acknowledges funding from the Scripps Seafloor Electromagnetic Methods Consortium.

References

Constable, S. C., R. L. Parker, and C. G. Constable [1987] Occam's inversion - A practical algorithm for generating smooth models from electromagnetic sounding data, *Geophysics*, 52(03), 289–300.

Du, Z. and Hosseinzadeh [2014] Seismic guided EM inversion in complex geology: Application to the Bressay and Bentley heavy oil discoveries, North Sea. 76th EAGE Conference and Exhibition, Expanded Abstract.

Key, K. [2012] Marine EM inversion using unstructured grids: a 2D parallel adaptive finite element algorithm, SEG Expanded Abstracts 1–5.

Newman, G. A., M. Commer, and J. J. Carazzone [2010] Imaging CSEM data in the presence of electrical anisotropy, *Geophysics*, 75(2), F51–F61, doi:10.1190/1.3295883.

Trefethen, L. N. [2000] *Spectral methods in MATLAB*, Society for Industrial and Applied Mathematics (SIAM), Philadelphia, PA.